www.czasopisma.pan.pl PAN POLSKA AKADEMIA NAUK www.journals.pan.pl

PAN ARCHIVES OF ACOUSTICS
Vol. 40, No. 1, pp. 11–18 (2015)

DOI: 10.1515/aoa-2015-0002

A Dedispersion Transform Method for Extracting the Normal Modes of a Shallow Water Acoustic Signal in the Pekeris Waveguide

Guang-Bing YANG[(1), (2), (3)], Lian-Gang LÜ[(3)], Da-Zhi GAO[(4)], Ying JIANG[(3)], Hong-Ning LIU[(3)]

[(1)] *South China Sea Institute of Oceanology, Chinese Academy of Sciences*
164, West XingangRoad, Guangzhou 510301, Guangdong Prov., P. R. China; e-mail: youngbingouc@gmail.com

[(2)] *University of Chinese Academy of Sciences*
19A, Yuquan Road, Beijing 100049, P. R. China

[(3)] *Key Laboratory of Marine Science and Numerical Modeling*
The First Institute of Oceanography, State Oceanic Administration
6, Xianxialing Road, Qingdao 266061, Shandong Prov., P. R. China

[(4)] *College of Information Science and Technology, Ocean University of China*
238, Songling Road, Qingdao 266100, Shandong Prov., P. R. China

(*received January 15, 2014; accepted October 1, 2014*)

The normal modes cannot be extracted even in the Pekeris waveguide when the source-receiver distance is very close. This paper introduces a normal mode extraction method based on a dedispersion transform (DDT) to solve this problem. The method presented here takes advantage of DDT, which is based on the waveguide invariant such that the dispersion associated with all of the normal modes is removed at the same time. After performing DDT on a signal received in the Pekeris waveguide, the waveform of resulting normal modes is very close to the source signal, each with different position and amplitude. Each normal mode can be extracted by determining its position and amplitude parameters by applying particle swarm optimization (PSO). The waveform of the extracted normal mode is simply the waveform of the source signal; the real waveform of the received normal mode can then be recovered by applying dispersion compensation to the source signal. The method presented needs only one receiver and is verified with experimental data.

Keywords: normal mode extraction, dedispersion transform, Pekeris waveguide, source ranging.

1. Introduction

Underwater acoustics are of great importance for studying the properties of water bodies and sediments (Makar, 2004; Grelowska *et al.*, 2013; Zhao *et al.*, 2013). In shallow water the sound pressure field can be described by a set of normal modes. Being able to extract each normal mode is very useful because each one contains information about the environment. With the information contained in the normal mode, the geoacoustic inversion (Bonnel *et al.*, 2010; 2012) can be conducted and information about the source (Nicolas *et al.*, 2006) can be obtained.

In this paper, a problem of an actual experiment is analyzed. This shallow-water propagation experiment was conducted in the Laoshan Bay of the Yellow Sea between 15th and 16th of August 2009. The water depth in the propagation path was about 18 m. The variance of the sound speed profile (SSP), shown in Fig. 1a, was less than 1 m/s. A magnetostrictive transducer with a central frequency of 820 Hz and an effective bandwidth of about 200 Hz was used as the source; its transmitting sensitivity was 185 dB re 1 μPa at 1 m. The source emitted a pseudo-noise phase-manipulated rank 10 M-sequence. The recorder was a 16-channel Sony-SIR-1000w sampled at 12 kHz. The signal was received using a 15 elements vertical line array (VLA) with 1 meter spacing located at distances of 1.39 km from the source. A matched filter technique was applied by performing autocorrelation to improve the signal-to-noise ratio (SNR). The source signal and original received signals with autocorrelation are shown in Fig. 1b and Fig. 2a.

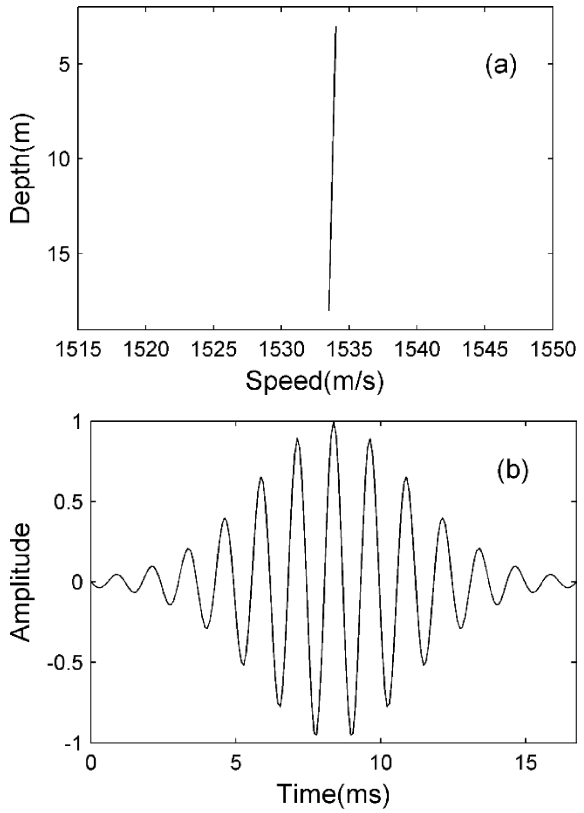

Fig. 1. The SSP and source signal (with autocorrelation) of the experimental data.

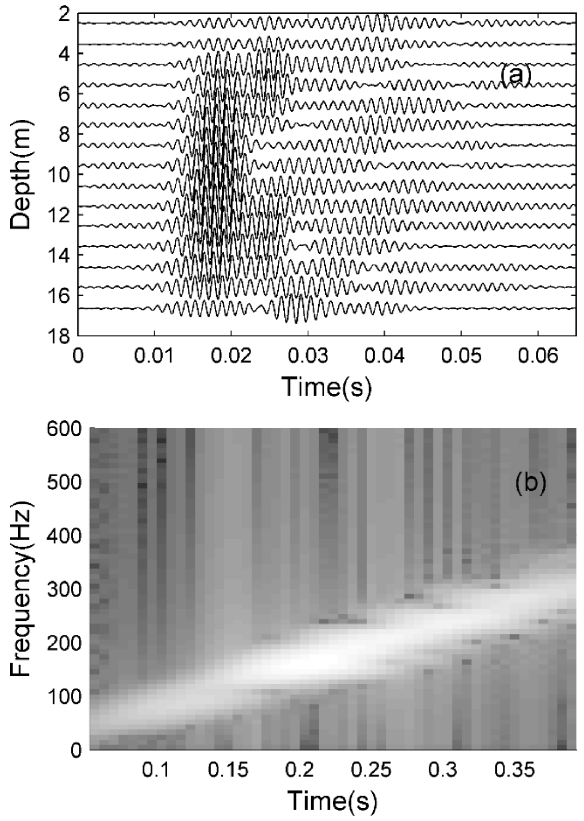

Fig. 2. The experimental data received at 1.39 km: a) the original signal from the VLA; b) the spectrogram of the signal received at depth 11m after time-warping.

The environment of the experiment is close to the Pekeris waveguide. Nevertheless, there is no method available to extract both the amplitude and the waveform of the normal mode in this very simple condition. The time-frequency analysis is a convenient way to show the normal mode distribution. The short time Fourier transform (STFT) is the most commonly applied time-frequency analysis method. The product of the time resolution (Δt) and the frequency resolution (Δf) of the STFT is a constant. That is, when the time resolution is improved, the frequency resolution decreases, and vice versa. Extracting normal modes using STFT is usually very difficult if the normal modes overlap. Many high resolution time-frequency methods have been developed (Huang *et al.*, 1998; Daubechies *et al.*, 2011). However, all these methods still have limited time-frequency resolution and cannot determine two substantially overlapped normal modes (Rilling, Flandrin, 2008; Wu *et al.*, 2011). In a study by Bonnel *et al.*, a warping transform is used to isolate the normal mode in spectrogram (Bonnel *et al.*, 2010; 2011; 2012). This warping method also relies on a time-frequency analysis with limited ability to separate normal modes as shown in Fig. 2b. The singular value decomposition (SVD) method (Neilsen *et al.*, 1997; Neilsen, Westwood, 2002) and the f-k transform (Walker *et al.*, 2005; Nicolas *et al.*, 2006) have been presented to extract the mode depth function or to isolate the normal mode in the frequency-wavenumber plane. The SVD can only extract the mode depth function. The f-k transform needs many samples at different ranges which are not available in this experiment.

Gao *et al.* (2010) suggested that the waveguide invariant β could be used to unify the horizontal wavenumber and remove the dispersion of each normal mode using one transform – the dedispersion transform. After DDT processing, the pulse length of each normal mode became as short as the pulse length of the source signal. In this work, the fact that after performing DDT on a signal received in the Pekeris waveguide is close to the superposition of a set of source signals with different positions and amplitudes is used. The position and amplitude parameters are determined with PSO (Kennedy, Eberhart, 1995), from which each normal mode can be extracted.

Section 2 of this paper presents normal mode extraction method based on the DDT. In Sec. 3, the results of applying this method on experimental signals are reported. The extracted normal modes are then used to estimate the source distance for further validation.

2. The normal mode extraction scheme

Normal mode extraction aims to identify the amplitude and waveform of each normal mode. In this paper,

normal mode extraction is conducted in two steps. The first step involves obtaining the amplitude of each normal mode, while the second step is to identify the waveform. Once the amplitude and position parameters are determined, the waveform of each normal mode can be identified using "dispersion compensation".

As introduced in the work of Gao *et al.* (2010), the dispersion of the received signal was removed after DDT processing, the pulse length of each normal mode became as short as the pulse length of the source signal. The experiment presented in this paper will show that the waveform of the received modes after applying DDT is the same as the waveform of the source signal in the Pekeris waveguide.

When considering the sound absorption α, the sound pressure can be written as

$$p(\omega, r, z) \approx S(\omega) \sum_{m=1}^{\infty} \psi_m(z_s)\psi_m(z) \frac{e^{ik_m r}}{\sqrt{k_m r}} \alpha_m(\omega), \quad (1)$$

where $\psi_m(z)$ is the normalized depth-dependent eigenfunction, k_m is the horizontal wavenumber, $S(\omega)$ is the source signal (Jensen *et al.*, 2011). Considering the shallow water Pekeris waveguide problem is discussed, density ρ is assumed to be depth independent for simplicity. The constant part is omitted for convenience. In the Eq. (1), the frequency-dependent terms are $S(\omega)$, $\psi_m(z)$, $1/\sqrt{k_m}$, and $\alpha_m(\omega)$. As Fig. 3 and Fig. 4 show, $1/\sqrt{k_m}$ and $\psi_m(z)$ change slowly with frequency in a certain bandwidth (this bandwidth is close to the bandwidth used in the experiment introduced in Sec. 1). If sound absorption is low, given that the source frequency is relatively low, then the change of sound absorption with frequency can also be omitted (Francois, Garrison, 1982).

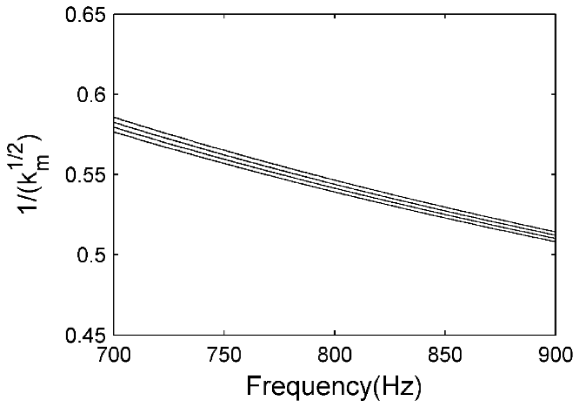

Fig. 3. The change of $1/\sqrt{k_m}$ $(m = 1, 2, 3, 4)$ with frequency.

In this case, Eq. (2) can be obtained with the help of DDT.

$$p\,(r, z; x, s) \approx \frac{1}{\sqrt{r}} \sum_{m=1} \frac{\alpha_m}{\sqrt{k_m}} \psi_m(z_s)\psi_m(z)$$

$$\left\{ \frac{1}{2\pi} \int_{-\infty}^{+\infty} \mathrm{d}\omega S(\omega) e^{i(\omega/c_0)(r-x)} e^{i(\omega^{-1/\beta}/c_0)(xs-r\eta_m)} \right\}. \quad (2)$$

As the dispersion term is removed and the frequency-independent terms α_m, $1/\sqrt{k_m}$, and $\psi_m(z_s)\psi_m(z)$ can be written as the mode-dependent

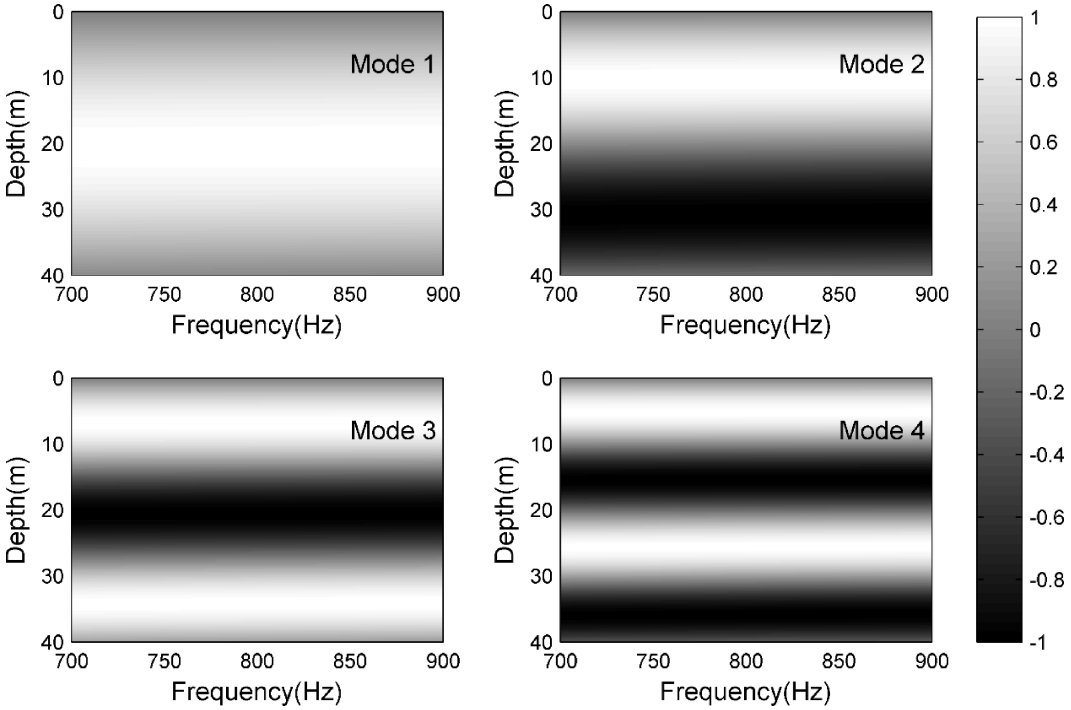

Fig. 4. The change of ψ_m (mode depth function) of modes 1, 2, 3, and 4 with frequency.

constant C_m, the range-dependent term is written as A_r, the received signal after DDT can be written as:

$$p(s) \approx A_r \sum_{m=1} C_m \{S(s - s_m)\}, \tag{3}$$

where s_m is the delay of each normal mode, and $S(s)$ is the source signal in the s domain. The existence of s_m in Eq. (3), due to the dispersion of each normal mode, is removed at different s values which places different normal modes at different positions after DDT.

After DDT processing of the received signal, the superposition of the source signals having different amplitudes and positions is an approximation of the resulting signal. If the relative amplitude and position of each normal mode can be determined, the received signal can then be reconstructed with source signal. The thick line at (1) in Fig. 5a shows a piece of the simulated received signal after DDT processing. The relative amplitude and position of each normal mode are easily determined by observation. The newly reconstructed signal (using the source signal) is in a good agreement with the original received signal after DDT processing. The correlation coefficient between them is over 0.98.

When the source-receiver distance is short, the normal modes will overlap even after applying DDT, as shown in Fig. 5b. Using the concepts presented above, the obtained signal after applying DDT to the received signal can be described using only the parameters of amplitude and position of each normal mode. In addition, those parameters can be determined using a searching process, which will allow the normal mode to be separated.

In this paper, the PSO is used to search for position and amplitude parameters. The PSO, initially inspired by animal behavior, can find the optimal value of an optimization function quickly and with small computational cost. The optimization function defined here is the correlation coefficient of the target signal (the received signal after DDT processing) and the reconstructed signal (the superposition of a set of source signals with different positions and amplitudes). The optimization parameters are the position and amplitude of each normal mode. When the maximum value of the correlation coefficient is found, the relative position and amplitude of each normal mode can be determined, and all of the normal modes can be extracted. Figure 5b shows the results of the parameter searching process. As the reconstructed signal becomes well correlated with the target signal (the correlation coefficient is generally above 0.9.), the amplitude and position parameters of each normal mode are determined. Each extracted normal mode agrees well with its corresponding separately simulated single mode.

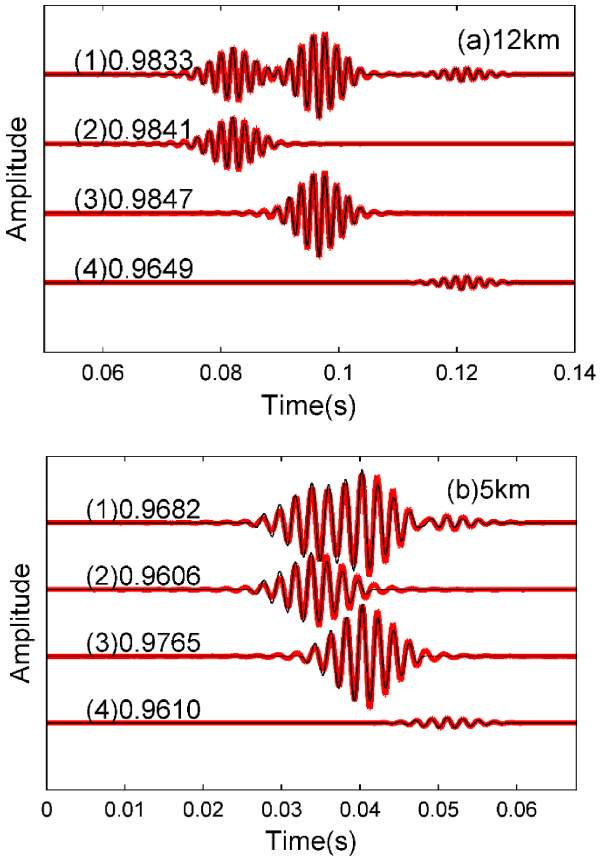

Fig. 5. The simulated received signal after DDT processing and its reconstruction using the source signal (the reconstructed signal). The data is received at 12 km (a) and 5 km (b) separately. The thick lines at positions (1), (2), (3), and (4) represent the simulated signal after DDT processing, showing the first three: the first, the second, and the third mode, respectively. The thin lines at (2), (3), and (4) represent the source signals with different positions and amplitudes determined by direct observation (a) and a PSO searching process (b) separately. The thin lines at (1) represent the combined thin lines at (2), (3), and (4). The correlation coefficients between overlapping thick and thin lines are labeled. (In this paper, the simulated signals are generated by employing the normal mode program Kraken with the environmental parameters shown in Table 1. Without loss of generality, only first three normal modes were considered in the simulation).

Table 1. Environmental parameters for simulation.

Water depth [m]	Sound speed of water [m/s]	Sound speed of sea bottom [m/s]	Density of sea bottom [kg/m^3]	Attenuation of sea bottom [dB/λ]	Source depth [m]
40	1500	1800	1900	0.2	15

Some problems may appear when conducting the searching process. First, the number of normal modes is usually not known without having some knowledge

of the environment, but this number can be determined with some attempts. For example, when the estimated number of normal modes is less than the actual number of normal modes, the correlation coefficient will not be very high. When the estimated number of normal modes is greater than the actual number of normal modes, there will be at least two normal modes that have the same position. Another problem involves determining the actual number of normal modes in a signal. Some modes may not be motivated at certain depths, so the total number of normal modes present can be different at different depths. To solve this problem, the signal transmitted and received by the transducers located at the bottom, where all the normal modes are motivated, can be used.

In addition to finding the actual number of normal modes, the SNR of the target signal needs to be relatively high to guarantee that the correlation coefficient will be high enough to accurately determine the optimization parameters using PSO. For this study, this requirement is satisfied because the studied signals are received relatively near the source.

Because the optimization function is defined as the correlation coefficient between the target signal and the reconstructed signal, the amplitude parameter of one mode needs to be fixed to avoid obtaining multiple optimal values. The mode with the fixed amplitude parameter should be the first mode because the amplitude sign of the first mode does not change with the depth (from the surface to the bottom). As dealing with the multi-channel signal, the relative amplitude of each channel needs to be determined because the amplitude parameter of the first mode is fixed. As shown in Fig. 7b, the front region of the first mode is not affected by the other modes. The amplitude of this region is used to determine the relative amplitude of each channel.

Along with the amplitude and position, the waveform of each normal mode must be considered. In this study, the recovered waveform is used to estimate the source distance, which is presented in Sec. 3. Previously, it has been proved that the time domain waveform of each normal mode after applying DDT is very close to the source signal. Consequently, the difference in waveform between the source signal and each normal mode of the received signal is mainly from the dispersion of the waveguide. Therefore, the dispersed received signal can be expressed as a function of the source signal:

$$S(t) \equiv \sum_{m=1} \frac{A_m}{2\pi} \int_{-\infty}^{+\infty} \mathrm{d}\omega S(\omega) e^{i(\omega/c_0)x - i\omega^{-1/\beta} x s_m / c_0}, \quad (4)$$

where $S(t)$ is the recovered received signal, and $S(\omega)$ is the source signal in the frequency domain. The exponential term and the amplitude term A_m are already known in the DDT process. The distance parameter x is the same for each mode, and the term s_m corresponds to the position parameters. By compensating the source signal with the dispersion, the real waveform of each normal mode can be obtained; it is called "dispersion compensation".

Figure 6 shows the recovered third normal mode waveform by applying dispersion compensation. The source signal is converted to the third normal mode by compensating the dispersion of the third normal mode. The recovered signal matches up well with the directly simulated signal as shown in Fig. 6b.

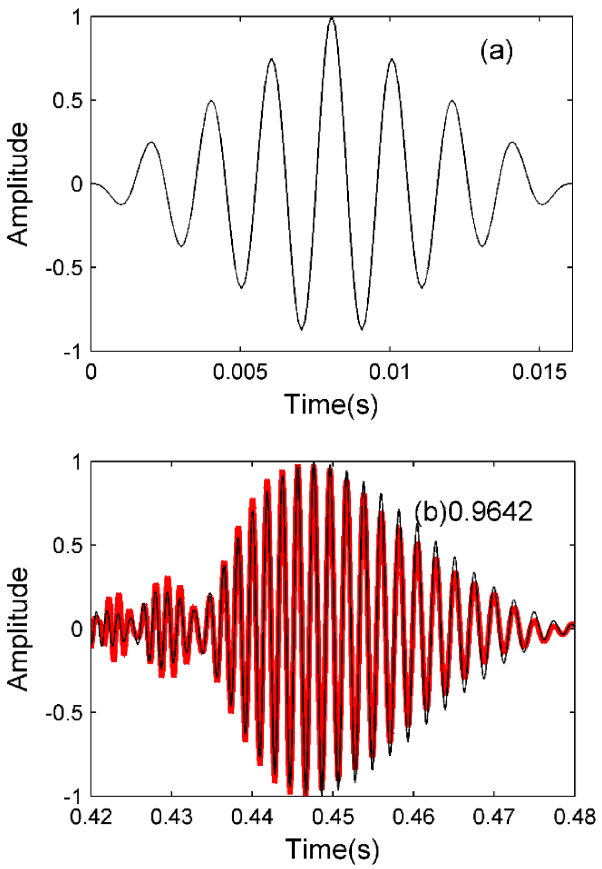

Fig. 6. Applying dispersion compensation to the simulated 3rd normal mode: a) the source signal; b) the thick line corresponds to the recovered signal, and the thin line corresponds to the directly simulated received signal (partially enlarged view). The correlation coefficient between these two overlapping lines is labeled.

3. Application and validation

In this section, experimental signals are used to highlight the usefulness of the presented method. The experimental data introduced in the Sec. 1 is used. The extracted modes are further used to estimate the source distance.

Zhao *et al.* (2010) introduced a broadband method to determine the distance from a source in shal-

low water using the Ω interference spectrum. This method takes advantage of the interference structure in the frequency domain caused by the third part of Eq. (6). At a certain distance r, the sound intensity will change with the frequency. In work presented by Zhao *et al.*, the period of the interference structure was used to estimate the source distance with

$$r_t = \frac{r_g \Delta\Omega_g}{\Delta\Omega_t}, \tag{5}$$

where $\Delta\Omega_g$ is the period of interference structure caused by the guide source, r_g is the distance of the guide source, and $\Delta\Omega_t$ is the period of the interference structure caused by the target source. This method determines the distance to the target source using only a single receiver and a broadband guide source. However, this method requires that the received signal consists of only two normal modes and the number of normal modes in the target signal and in the guide signal must be the same in order to confirm that the difference of wavenumber is the same. Because the period of the interference structure changes with frequency and more than two modes may make up the received signal, this method cannot be that accurate.

With the method presented in this paper, the normal modes are first able to be separated. Then, two modes are chosen and their actual received waveforms are recovered using dispersion compensation. The acoustic intensity of these two modes can be written as

$$I(r, z, z_s, \omega) = A^2(\omega)\left(B_n^2 + B_m^2 + 2B_n B_m \cos\left(k_{mn}(\omega) r\right)\right), \tag{6}$$

where $A^2(\omega)$ is the power spectrum of the source signal, B_n and B_m are the normal mode amplitude, r is the distance between source and receiver (Jensen *et al.*, 2011). The interference structure in the frequency domain caused by $\cos(k_{mn}(\omega)r)$ is shown in Fig. 8a, c. Using a simple operation, Eq. (6) can be rewritten as

$$\cos\left(k_{mn}(\omega) r\right) = \frac{\dfrac{I(r, z, z_s, \omega)}{A^2(\omega)} - B_n^2 - B_m^2}{2B_n B_m}. \tag{7}$$

The interference structure is more clearly shown in Fig. 8b, d. As expressed in Eq. (7), the distance r corresponds to the phase change of the interference structure. The distance of the target source can be obtained using

$$\frac{\Delta p_t}{\Delta p_g} = \frac{r_t \Delta k_{mn}(\omega)}{r_g \Delta k_{mn}(\omega)} = \frac{r_t}{r_g}, \tag{8}$$

where Δp_t and Δp_g are the phase change of the interference structure corresponding to the target source and the guide source, respectively. Compared with Eq. (5), Eq. (8) is more accurate because $\Delta\Omega_g$ and $\Delta\Omega_t$ correspond to different frequency scales, while Δp_t and Δp_g in Eq. (8) correspond to the same frequency scale.

Using DDT and the parameter searching process, the first six normal modes of the experimental signal are extracted. All six normal modes become distinguishable in Fig. 7b. The vertical distribution of the sixth mode is not clear due to the spatial resolution limit (only 15 hydrophones on the VLA).

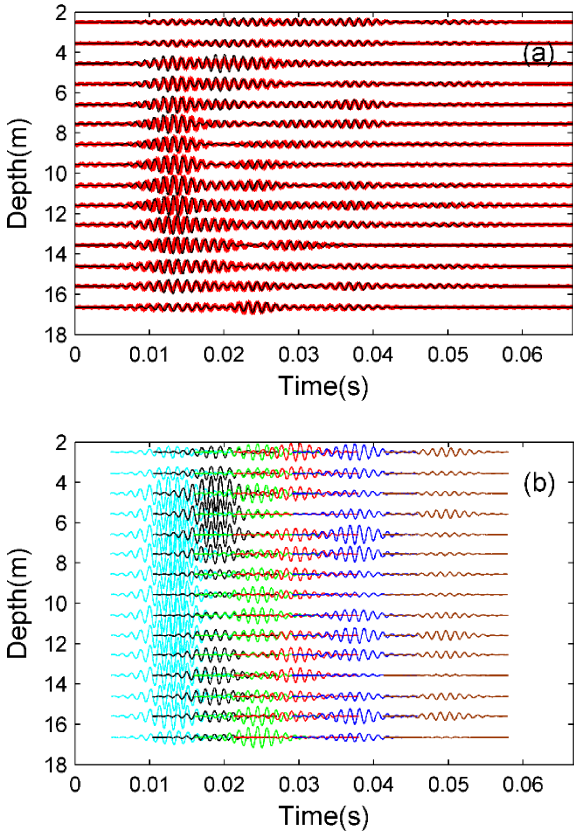

Fig. 7. Extracting normal modes from experimental data received at 1.39 km: a) the thin line corresponds to the signal after applying DDT, and the thick line corresponds to the reconstructed signal, with extracted modes shown in (b); b) the extracted normal mode.

The extracted 1st and 2nd normal modes are recovered to give the actual received waveform using dispersion compensation, and they are added to observe the interference structure in the frequency domain as shown in Fig. 8a,c. With the application of Eq. (7), the interference structure is extracted and the corresponding phase change is obtained as shown in Fig. 8(b, d, and e). The data at 4.63 km is assumed to be the guide signal, giving a calculated target source distance of 1.27 km, while the actual distance is about 1.39 km.

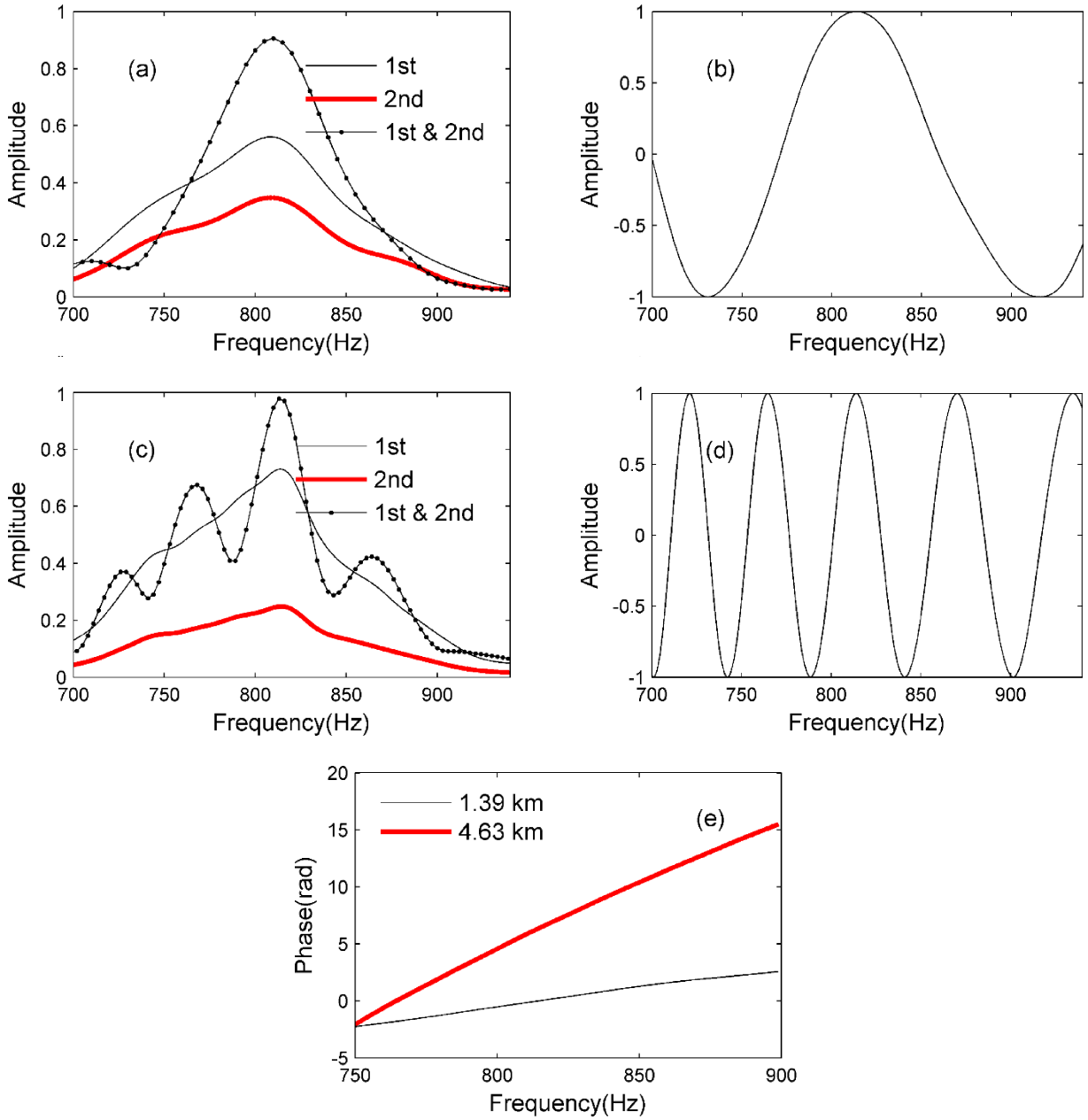

Fig. 8. Extracting the Ω interference structure of two normal modes and the corresponding phase change using experimental data: (a, c) spectrum of the 1st and 2nd modes and their compositions received separately at 1.39 km and 4.63 km; (b, d) the extracted interference structures in the frequency domain using Eq. (7); (e) the corresponding phase changes of (b, d).

4. Conclusions

This study presents a normal mode extraction method based on DDT to solve a problem raised in an experiment. In the Pekeris waveguide, the dispersion of a received signal can be removed with DDT, and the received signal then becomes the composition of source signal having different amplitudes and positions. The amplitude and position parameters can be determined using a PSO searching process. Once the amplitude and position parameters have been determined, the normal modes can be separated. With the introduction of dispersion compensation, the original waveform of the received normal mode can be recovered by compensating the dispersion to the source signal.

Using the relationship between the normal modes based on the waveguide invariant, the method presented here can extract normal modes that otherwise cannot be distinguished using other methods. Given the extracted normal modes, the source distance can be estimated by observing the Ω interference structure which further validate the usefulness of the presented method. As the environment is usually range depen-

dent, the geoacoustic and other applications can get more accurate results when the normal mode information can be extracted at relative close source-receiver range. That is the main significance of this method.

The method developed is tested using experimental conditions obtained from Yellow Sea experiments. However, this method requires the source signal to be known and is only applied in the Pekeris waveguide where the $\beta \approx 1$. When there is a strong thermocline, the distribution of normal modes becomes more complex. In this case, the waveguide invariant β varies with frequency and the DDT does not work properly.

Acknowledgments

The author would like to thank Dr. Xianyao Chen for his many useful suggestions. Financial support for this research was provided by the Public Science and Technology Research Funds Projects of Ocean, under Grant No. 201005004-02. This work was also supported by the National Natural Science Foundation of China, under Grant No. 40806015 and No. 41006020.

References

1. Bonnel J., Nicolas B., Mars J.I., Walker S.C. (2010), *Estimation of modal group velocities with a single receiver for geoacoustic inversion in shallow water*, Journal of the Acoustical Society of America, **128**, 2, 719–727.
2. Bonnel J., Gervaise C., Roux P., Nicolas B., Mars J.I. (2011), *Modal depth function estimation using time-frequency analysis*, Journal of the Acoustical Society of America, **130**, 1, 61–71.
3. Bonnel J., Gervaise C., Nicolas B., Mars J.I. (2012), *Single-receiver geoacoustic inversion using modal reversal*, Journal of the Acoustical Society of America, **131**, 1, 119–128.
4. Daubechies I., Lu J., Wu H. (2011), *Synchrosqueezed wavelet transforms: an empirical mode decomposition-like tool*, Applied and Computational Harmonic Analysis, **30**, 2, 243–261.
5. Francois R.E., Garrison G.R. (1982), *Sound absorption based on ocean measurements. Part II: Boric acid contribution and equation for total absorption*, Journal of the Acoustical Society of America, **72**, 6, 1879–1890.
6. Gao D.Z., Wang N., Wang H.Z. (2010), *A Dedispersion Transform for Sound Propagation in Shallow Water Waveguide*, Journal of Computational Acoustics, **18**, 3, 245–257.
7. Grelowska G., Kozaczka E., Kozaczka S., Szymczak W. (2013), *Underwater noise generated by a small ship in the shallow sea*, Archives of Acoustics, **38**, 3, 351–356.
8. Huang N.E., Shen Z., Long S.R., Wu M.C., Shih H.H., Zheng Q., Yen N., Tung C.C., Liu H.H. (1998), *The empirical mode decomposition and the Hilbert spectrum for nonlinear and non-stationary time series analysis*, Proceedings of the Royal Society of London. Series A: Mathematical, Physical and Engineering Sciences, **454**, 1971, 903–995.
9. Jensen F.B., Kuperman W.A., Porter M.B., Schmidt H. (2011), *Computational ocean acoustics*, Springer, New York.
10. Kennedy J., Eberhart R. (1995), *Particle swarm optimization*, Proceedings of IEEE International Conference on Neural Networks, pp. 1942–1948, Perth.
11. Makar A. (2004), *Estimation of the time delay of hydroacoustic signals for passive location of underwater objects*, Archives of Acoustics, **29**, 3, 435–445.
12. Neilsen T.B., Westwood E.K., Udagawa T. (1997), *Mode function extraction from a VLA using singular value decomposition*, Journal of the Acoustical Society of America, **101**, 5, 3025.
13. Neilsen T.B., Westwood E.K. (2002), *Extraction of acoustic normal mode depth functions using vertical line array data*, Journal of the Acoustical Society of America, **111**, 2, 748–756.
14. Nicolas B., Mars J.I., Lacoume J. (2006), *Source depth estimation using a horizontal array by matched-mode processing in the frequency-wavenumber domain*, EURASIP Journal on Applied Signal Processing, **2006**, 65901, 1–16.
15. Rilling G., Flandrin P. (2008), *One or two frequencies? The empirical mode decomposition answers*, IEEE Transactions on Signal Processing, **56**, 1, 85–95.
16. Walker S.C., Roux P., Kuperman W.A. (2005), *Data-based mode extraction with a partial water column spanning array*, Journal of the Acoustical Society of America, **118**, 3, 1518–1525.
17. Wu H., Flandrin P., Daubechies I. (2011), *One or two frequencies? The synchrosqueezinganswers*, Advances in Adaptive Data Analysis, **3**, 01&02, 29–39.
18. Zhao D., Huang Z., Su S., Li T. (2013), *Matched-eld source localization with a mobile short horizontal linear array in offshore shallow water*, Archives of Acoustics, **38**, 1, 105–113.
19. Zhao Z., Wang N., Gao D., Wang H. (2010), *Broadband source ranging in shallow water using the Ω-interference spectrum*, Chinese Physics Letters, **27**, 6, 064301.